

Phaeodactylum tricornutum as a source of value-added products: A review on recent developments in cultivation and extraction technologies

Original

Phaeodactylum tricornutum as a source of value-added products: A review on recent developments in cultivation and extraction technologies / Celi, C.; Fino, D.; Savorani, F.. - In: BIORESOURCE TECHNOLOGY REPORTS. - ISSN 2589-014X. - ELETTRONICO. - 19:(2022), p. 101122. [10.1016/j.biteb.2022.101122]

Availability:

This version is available at: 11583/2970170 since: 2022-07-19T09:10:49Z

Publisher:

Elsevier

Published

DOI:10.1016/j.biteb.2022.101122

Terms of use:

This article is made available under terms and conditions as specified in the corresponding bibliographic description in the repository

Publisher copyright

Elsevier postprint/Author's Accepted Manuscript

© 2022. This manuscript version is made available under the CC-BY-NC-ND 4.0 license
<http://creativecommons.org/licenses/by-nc-nd/4.0/>. The final authenticated version is available online at:
<http://dx.doi.org/10.1016/j.biteb.2022.101122>

(Article begins on next page)

26 successful biorefinery extraction cascades experimented on this diatom are described to
27 foster research in this direction.

28 **Keywords:** *Phaeodactylum tricornutum*; algal cultivation; extraction technologies;
29 value-added products; biorefinery concept

30 **1. Introduction**

31 The climate change consequences that we are forced to face nowadays demand urgent
32 change in society, especially in the manufacturing and transport sectors. There is a need
33 to replace petroleum-based commodities and fuels with biobased ones before the
34 consequence of industrialization will become overwhelming for our planet.

35 Recent political strategies have been implemented to facilitate the transition to a circular
36 bioeconomy model, able of ensuring both economic growth and preservation of natural
37 resources. Hope and effort in this sense have been placed on microalgae, key players in
38 blue biotechnology because they can offer a significant contribution to the building of
39 this sustainable economy model by providing both low-value and high-volume
40 products, and high-value and low-volume products.

41 Beyond the several microalgae strains that are currently studied at a research level,
42 industrial-scale cultivations have also arisen to exploit the intrinsic capacity of some
43 strains to accumulate specific metabolites, like β -carotene from *Dunaliella salina* or
44 astaxanthin from *Haematococcus pluvialis*, not to mention the long-established use of
45 algae as a food ingredient in the Asiatic continent.

46 The present review proposes a literature collection on *Phaeodactylum tricornutum*, a
47 model diatom, which has been already examined at a laboratory scale and whose
48 industrial potential has been revealed. The ultimate scope is to provide the optimal
49 cultivations conditions that have arisen from numerous studies conducted through the

50 years and how these influence the final biochemical composition and its consequent
51 applicability.

52 **1.1 Diatoms overview**

53 Diatoms are single-celled algae belonging to the group of eukaryotic phytoplankton that
54 have existed for more than 180 million years. Present in many areas of the world, they
55 are particularly widespread at high latitudes and in coastal ecosystems rich in nutrients
56 (Malviya et al., 2016). They can have radial symmetry, in the case of centric diatoms, or
57 bilateral symmetry as for pennate diatoms. These unicellular photosynthetic organisms,
58 sizing from 1 μm to 200 μm , undertake significant roles in the major biogeochemical
59 cycles, such as carbon sequestration, oxygen production, and nutrient recycling,
60 especially nitrogen, carbon, and silicon. About 20% of global carbon fixation can be
61 indeed ascribed to diatoms (Hockin et al., 2012) which produce, through their
62 photosynthetic apparatus, more than 20% of the world's oxygen production.
63 Furthermore, they provide a large amount of organic matter, about 25% of global
64 biomass production, thus supplying nourishment to most other aquatic organisms (Not
65 et al., 2012).

66 Given their global distribution, diatoms present high variability and diversification.
67 Researchers often attempted to estimate the numbers of diatom species through time:
68 the latest values are from 1800 planktonic species to 200000, more than any other single
69 algal class. Because of their complex evolutionary history and genomic reorganization,
70 diatoms have developed a range of potentially useful features, such as a rigid silicified
71 cell wall called frustule, vacuoles for nutrient storage, fast reactions to changes in
72 environmental conditions, resting stage formation, ice-binding proteins, and a urea cycle
73 (Malviya et al., 2016).

74 The frustules are constituted of silicic acid and other organic materials, whose
75 morphology may vary according to environmental factors and cell condition. The
76 presence of silica in diatoms has also been related to the formation of diatomite, which
77 has been commercially mined for many uses. Indeed, along geological periods, diatoms'
78 death and decomposition entail the formation of sediments of silicon on the seafloor,
79 which constitutes this diatomaceous earth or diatomite (Branco-Vieira et al., 2018).

80 Other valuable and interesting metabolites can be found in diatom chloroplasts, such as
81 chlorophyll *a*, *c1*, and *c2*, and a complement of accessory pigments, including
82 xanthophylls and carotenes. The light-harvesting pigments chlorophyll *a*, chlorophyll *c*,
83 and fucoxanthin together constitute the complex fucoxanthin-chlorophyll protein (FCP),
84 which has the function of harvesting the light necessary for diatoms. The pigment
85 fucoxanthin is also responsible for the golden-brown color of these microalgae, being
86 the most abundant pigment. Nowadays, seaweeds represent the main source of
87 fucoxanthin at industrial scale. Nevertheless, marine diatoms accumulate 5-10 fold
88 higher amounts (2.24 to 26.6 mg g⁻¹ DW) and thereby are regarded as a potential source
89 of this valuable pigment (Pereira et al., 2021).

90 Carotenoids instead are involved in cell photoprotection when the variability in light
91 intensity, typical of the marine ecosystem, threatens to assimilate overmuch light energy
92 and, consequently, may compromise photosynthetic productivity through a mechanism
93 called photoinhibition. This process, occurring when light energy is absorbed beyond
94 the photosynthetic capacity of the cell, involves the production of reactive oxygen
95 species (ROS) like hydroxyl radicals (OH•), superoxide anions (O₂⁻), hydrogen
96 peroxide (H₂O₂), and singlet oxygen (¹O₂), that can provoke the oxidization of any
97 pigment, lipid, or protein nearby, thus damaging the photosynthetic apparatus (Jallet et

98 al., 2016). To prevent photoinhibition diatom cells have developed an assortment of
99 defence tools, such as the diadinoxanthin cycle associated with diadinoxanthin de-
100 epoxidation and diatoxanthin epoxidation. The latter is indeed directly involved in the
101 dissipation of energy through the action of Non-Photochemical Quenching (NPQ),
102 which allows the photoacclimation of the light-harvesting system (Kooistra et al.,
103 2007). The presence of diadinoxanthin, diatoxanthin, and additionally violaxanthin,
104 antheraxanthin, and zeaxanthin can be noted especially in cells subjected to excessive
105 light energy (Kuczynska et al., 2020).

106 Lipids and carbohydrates instead represent energy storage metabolites. In particular,
107 carbohydrates can be sorted into insoluble and soluble. The first ones are structural
108 carbohydrates that are frustule-associated sugars, such as sulphated glucoromannans,
109 callose, and chitin; whereas, soluble carbohydrates are chrysolaminarin,
110 exopolysaccharides or extracellular polysaccharides (EPS), and free sugars (Caballero
111 et al., 2016). Among polysaccharides, chrysolaminarin constitutes the preferred energy
112 storage for diatoms and normally accounts for 10-20% of the total carbon in cells at the
113 exponential stage (Kroth et al., 2008). It is constituted of a backbone of β -1,3-D-glucose
114 units linked together, with a degree of branching of 0-0.2 at position 6 and a degree of
115 polymerization of 5-60. Its accumulation occurs in vacuoles inside the cell during the
116 photosynthetically active light periods, while it is consumed in the dark to fuel
117 heterotrophic metabolism (Caballero et al., 2016).

118 Regarding the lipidic fraction, different types of lipids can be detected in these
119 microalgae: fatty acids, polar lipids, non-polar lipids, triacylglycerides (TAGs), steroids,
120 and oxylipins. Diatoms' cell membrane is predominantly composed of fatty acids,
121 which comprise between 15 and 25% of their biomass. Common in diatoms are the

122 saturated fatty acid myristic acid (C14:0) and palmitoleic acid (C16:1), belonging to
123 monounsaturated fatty acids (MUFAs). Polyunsaturated fatty acids (PUFAs) are instead
124 composed of 18-22 carbon chains with two or more double bonds. Stearidonic acid
125 (SDA, 18:4), α -linolenic acid (ALA, 18:3), eicosapentaenoic acid (EPA, 20:5) and
126 docosahexaenoic acid (DHA, 22:6) belong to ω -3 PUFAs group; while ω -6 PUFAs are
127 for example arachidonic acid (ARA, 20:4) and γ -linoleic acid (GLA, 18:3). PUFAs,
128 particularly the ω -3 category, have gained great visibility through the years thanks to
129 their role as bioactive substances and as essential nutrients promoting human health.
130 The relative amounts of storage carbon that accumulate in lipids and carbohydrates can
131 be modified by altering the cell's physiological condition as a result of the breakdown
132 of some biosynthetic pathways and the activation of new ones, involving increased
133 production of lipids or carbohydrates. For example, nitrogen depletion has been a
134 widely tested strategy to manipulate algal metabolism with the intent of favoring lipids
135 production. It was also argued that a boosted production of TAG can be stimulated by
136 blocking the polysaccharides metabolism through genetic engineering, as the resulted
137 unplaced storage carbon would be relocated to other storage metabolites, in this case,
138 lipids. (Caballero et al., 2016).

139 Hence, it is evident how diatoms can be a potential feedstock for numerous
140 biotechnological purposes and an extensive line of applications in industry. Besides
141 their interesting biochemical composition and ability to produce valuable metabolites,
142 they exhibit a high capacity to thrive in both fresh and marine water and do not require
143 fertile lands, if compared to biomass produced by terrestrial crops. Moreover, they
144 rapidly adapt to changing nutrient conditions and provide high biomass production
145 rates. Despite these advantages, their commercialization and industrialization still lack

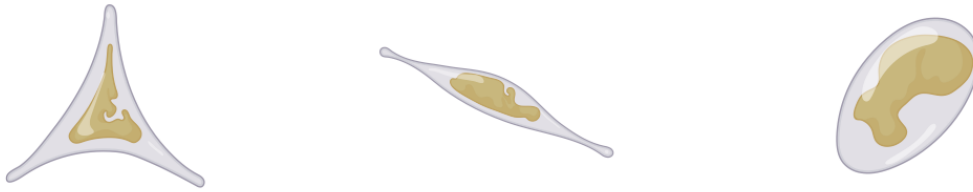
146 to be standardized at a large scale, mainly due to regulatory and technological barriers,
147 such as the high water, energy, and nutrients consumption during the cultivation step
148 and some technical hindrances to biomass recovery. Currently, the industrial production
149 of microalgae for commercial purposes is related to a cost of 3.4 € kg⁻¹ for a
150 hypothetical Spanish production plant (Penhaul Smith et al., 2020). However,
151 production costs are subjected to variations depending on different factors, including the
152 cultivation system (photobioreactors or open ponds), costs associated with workforce,
153 operating costs, etc. Therefore, the gaps in the realization of large-scale cultivation,
154 such as plant capability and dimension, and standardization of cultivation methods must
155 be filled. The limits in the commercialization of high-value products need to be
156 overcome by testing cheap and sustainable extraction technologies. Moreover, further
157 studies are essential in the optimization of downstream processing leading to multiple-
158 compound production in a biorefinery concept, which could ultimately enhance the
159 economic viability.

160 **1.2 Properties and Potential of *Phaeodactylum tricornutum***

161 Among marine diatoms, *Phaeodactylum tricornutum* is one of the species examined to
162 the highest extent and whose genome has been completely sequenced in 2008. It is a
163 marine pennate diatom and belongs to the brown-algae division of Bacillariophyceae of
164 Heterokontophyta. It contains about 36.4% of proteins, 26.1% of carbohydrates, 18.0%
165 of lipids, and 15.9% of ash on dry weight, under ordinary cultivation conditions (Zhang
166 et al., 2018). *P. tricornutum*, growing in brackish to saline water in several locations of
167 the world, owns the peculiar feature to be polymorphic, thus exhibiting three principal
168 morphotypes: oval, triradiate, and fusiform (**Figure 1**). Evidence is also present that a

169 fourth rarer morphotype exists, called cruciform, favoured by low temperatures, and
170 converting to the oval type through the degeneration of arms (He et al., 2014).
171 As a consequence of fluctuations in growth conditions, especially culture medium,
172 salinity, pH, and temperature, the cells are subjected to reversible morphological
173 conversions from one form to another. For instance, suboptimal conditions such as low
174 temperature, hyposalinity, low light intensity, and nutrient limitation resulted to
175 stimulate oval cell formation. Song et. al (2020) characterized ten strains of *P.*
176 *tricornutum* and reported that Mann and Myers' medium favours morphotype transition
177 from fusiform to oval, while the prevalence of fusiform cells was observed in f/2
178 medium. Biochemical analysis proved that oval morphotype accumulated higher protein
179 and pigments content, whereas lipids and carbohydrates were more abundant in
180 fusiform cells. However, the latter exhibited a higher maximum specific growth rate
181 (0.76 d^{-1} against 0.43 d^{-1} ; doubling time 0.92 d against 1.65 d) (Song et al., 2020).
182 Thereby this study opens up the possibility of selectively growing a certain morphotype
183 when specific final characteristics are desired for a particular industrial application.
184 Oval cells are also characterized by harder walls (Young modulus equal to 500 kPa)
185 compared to the other types (100 kPa) (Francius et al., 2008) and by siliceous frustules
186 when silicic acid is included in the growth medium. Nonetheless, silicified substances
187 are not indispensable for *P. tricornutum*, which can effectively reproduce also in
188 absence of silica. Differences have been noted when comparing silicified fractions of
189 the triradiate and fusiform with those of the oval type: fusiform and triradiate cells are
190 characterized by silica bands; while only the oval ones hold silica valves typical of
191 diatoms (Tesson et al., 2009).
192

193



194

195 **Figure 1.** Morphotypes of *Phaeodactylum tricornutum* from left to right: triradiate,

196 fusiform, oval. (Created with Biorender)

197

198 Among other properties, *P. tricornutum* presents a high ability for the Non-
199 Photochemical Quenching (NPQ) that dissipates the excess light in form of heat. This
200 capacity was tested by using a sinusoidal light scheme for its cultivation and the
201 outcome was that this diatom exhibited minimal indications of photoinhibition. Damage
202 by photoinhibition can be measured as photosynthetic capability by the maximal
203 quantum yield (F_v/F_m) of photosynthetic system II (PSII), where F_m indicates
204 the maximal fluorescence level and F_v is the variable fluorescence obtained by
205 subtracting F_o (minimal fluorescence) to F_m (Jallet et al., 2016; Murchie and Lawson,
206 2013). The study of Huete-Ortega et al. (2018) shows that light irradiance above 400-
207 500 $\mu\text{mol photons m}^{-2} \text{s}^{-1}$ saturated PSII activity of *P. tricornutum*, independently of
208 nitrogen-replete or -deplete conditions. Moreover, the NPQ response was not activated
209 until approximately 200 $\mu\text{mol photons m}^{-2} \text{s}^{-1}$ irradiance; therefore, an optimal light
210 intensity of 213 $\mu\text{mol m}^{-2} \text{s}^{-1}$ was found for *P. tricornutum* in N-replete mode (Huete-
211 Ortega et al., 2018).

212 An industrially relevant feature of *P. tricornutum* is that it is a fast-growing species,
213 which makes it suitable to be cultivated at a large scale. To date, in Europe, it is
214 cultivated by at least eight companies reaching a yearly production of 4 tons of dry
215 biomass (Araújo et al., 2021). Among them, *P. tricornutum* is exploited for fucoxanthin
216 production by AlgaTechnologies (Israel) and for EPA production by Simris (Sweden).
217 Moreover, *P. tricornutum* extract and EPA-rich oil extract were proposed for
218 authorization as novel food to the European Union, whose evaluations are still ongoing.
219 This diatom presents a strong adaptation to a wide assortment of culture media,
220 including Walnes, f/2, COMBO, M&M, and enriched seawater. It tolerates high
221 pH/light intensities albeit growing also under poor light conditions (Butler et al., 2022).

222 In addition, it can be genetically transformed, and the employment of different genetic
223 manipulations showed promising results in increasing lipid content. However, the
224 exploitation of diatoms' lipids for biofuel production is far to be economically
225 competitive on the market; thereby, priority should be given to multiple high-value
226 compound production. The valorisation of all biomass components by extracting
227 multiple algae metabolites, can improve the economic feasibility of this value chain and
228 promote their industrial application (Branco-Vieira et al., 2020).

229 Even if less commercially competitive, healthful substances obtained from microalgae
230 own specific advantages over standard synthetic alternatives: from a chemical point of
231 view, synthetic molecules are only present in specific isomers, which are normally
232 much less effective than natural versions for certain applications, such as in artificial
233 milk, dietary supplements or fish pigment enhancers (Enzing et al., 2014). PUFAs such
234 as EPA and DHA have been shown to improve eye health, and brain development, and
235 perform cardiovascular and inflammatory disease prevention, anti-aging function, and
236 treatment of psychiatric disorders. Currently, deep ocean fish oil represents the primary
237 feedstock for EPA and DHA production; however, unpleasant smell, environmental
238 impacts to the marine ecosystem due to overfishing, heavy metals toxicity, and
239 considerable purification needs demanded sustainable fatty acids production alternatives
240 (Kadalag et al., 2021). Moreover, only 0.2 million tons of EPA/DHA are obtained from
241 fish sources, in the face of 1.3 million tons required for the world population, given the
242 500 mg/day intake recommended by the World Health Organization (Wang et al.,
243 2021). Hence, further studies to increase fatty acids accumulation in microalgae
244 biomass are needed to facilitate their industrial application. Fucoxanthin also exerts
245 multiple pharmacological bioactivities including anti-inflammatory, anti-obesity, anti-

246 diabetic effects, anti-cancer, and antioxidant (Song et al., 2020). Anti-tumor
247 bioactivities were determined also in chrysolaminarin (Zhang et al., 2018).

248 **2. Cultivation strategies**

249 Microalgae are generally considered to be obligate photoautotrophs, by using sunlight
250 and converting CO₂ to reduced carbon, thus producing oxygen and chemical energy
251 through photosynthesis (Penhaul Smith et al., 2020). This encompasses a series of
252 biochemical redox reactions which convert light energy into chemical energy in the two
253 photosystems, PSI and PSII. The ATP and the reducing power (NADPH), resulting
254 from the electron transport chain, are then metabolized in the Calvin–Benson–Bassham
255 cycle (CBB) by the Rubisco enzyme (Villanova et al., 2017). Nevertheless, many
256 microalgae can assimilate organic nutrients and grow in the dark by respiration or
257 fermentation of exogenous sugars through *heterotrophy*. If the species can switch
258 between heterotrophy and *phototrophy*, or employs both respiration and photosynthesis,
259 then the cultivation is carried out in *mixotrophy*. However, the provision of an organic
260 carbon compound will induce a variation in the cell carbon partitioning with relative
261 consequences on metabolic pathways, growth phase, and final biochemical composition
262 (Penhaul Smith et al., 2020).

263 Even if microalgae production through phototrophy could be a cheap process since only
264 light energy is exploited, this cultivation mode entails some limitations such as the
265 scarce maximum biomass production achievable because of self-shading effects and the
266 subsequent drawbacks in optimizing temperature control, gas/liquid ratio, and light
267 penetration. On the other hand, mixotrophy is considered a viable alternative to obtain
268 high biomass productivity, considering the lower demand for light penetration.
269 Moreover, by employing cheap and easily accessible organic carbon sources, including

270 wastewaters, the economic feasibility of the process can be even further enhanced
271 (Villanova et al., 2021). The selection of the cultivation mode, and subsequently of the
272 carbon sources in the case of mixotrophy and heterotrophy, depends on the species and
273 the bioproducts of interest. Indeed, if PUFAs production through heterotrophy is
274 feasible, the same can not be achieved for pigments since the production of
275 photosynthesis-related compounds is strictly associated with the presence of light and it
276 is thereby nullified in heterotrophic cultures (Cerón-García et al., 2013, 2005). In
277 addition, some species could not be able to operate heterotrophic growth through dark
278 sugar fermentation, which is the case of *P. tricornutum* which can be grown
279 heterotrophically only upon metabolic engineering (Villanova et al., 2021).

280 **2.1 Phototrophic cultivation of *Phaeodactylum tricornutum***

281 Several photobioreactors (PBRs) types such as flat-plate, bubble-columns, and tubular,
282 have been designed and tested to cultivate *P. tricornutum* phototrophically. Among
283 these, flat-panel configurations have proven to accomplish low shear stress and
284 adequate irradiation which ultimately resulted in higher biomass, EPA, and fucoxanthin
285 productivities. Illumination constitutes a primary affecting element in biomass
286 production and biochemical composition, together with light wavelength and light:dark
287 cycle. The increase of light intensity usually involves the rise of the growth rate until it
288 reaches a saturation value. Nonetheless, above this saturation value, the growth is
289 inhibited by the production of harmful substances (i.e., ROS), involved in the
290 photoinhibition process, which eventually cause a decrease in biomass productivity
291 (Villanova et al., 2021). Generally, the photosynthetic efficiency in microalgae grown in
292 phototrophic conditions is lower than theoretically achievable values, due to the
293 complex nature of the culture system, in which various parameters influence differently

294 the growth and the biochemical composition, resulting in countertrend effects. (Butler et
295 al., 2020). Maximum biomass productivities achieved with *P. tricornutum*, and the
296 productivity of different target compounds obtained in phototrophic cultures are
297 reported in **Table 1** and **Table 2**, respectively.

298

Strain	Medium	Photobioreactor design	Maximum biomass productivity	Reference
UTEX 640 and UTEX 646	f	Green wall panel III (≤ 40 L) outdoor	$17.80 \text{ g m}^{-2} \text{ day}^{-1}$ (nitrogen-replete culture)	(Gilbert-López et al., 2015)
FACHB-Collection	f/2	Indoor bubble columns photobioreactors (3 L)	$227.09 \text{ mg L}^{-1} \text{ day}^{-1}$	(Rodolfi et al., 2017)
UTEX 640	ASW	Outdoor parallel photobioreactors (51 L)	$> 0.3 \text{ mg L}^{-1} \text{ day}^{-1}$	(Song et al., 2014)
		PVC circular outdoor pond	$\sim 0.15 \text{ mg L}^{-1} \text{ day}^{-1}$	
EPSAG-Collection	f/2	Greenhouse PBR phytobags (3000 L)	$7.62 \text{ g m}^{-2} \text{ day}^{-1}$	(Silva Benavides et al., 2013)
CCAP 1055/1	Cell-Hi JWP	Indoor Airlift glass tubular photobioreactor (ALR) PhycoLift (8 L)	$1.57 \text{ g L}^{-1} \text{ day}^{-1}$	(Wang et al., 2018)
		Outdoor Airlift glass tubular photobioreactor (ALR) PhycoLift (8 L)	$0.93 - 1.13 \text{ g L}^{-1} \text{ day}^{-1}$	

299

300 **Table 1.** Biomass productivity of *P. tricornutum* strains in various photosynthetic
301 systems.

302

Product class	Product	Strain	Product yield / productivity	Operational conditions	Reference
Lipids	EPA	EPSAG-Collection	280 mg m ⁻² day ⁻¹ 3.68% DW	Greenhouse PBR phytobags (3000L)	(Butler et al., 2022)
		CCAP 1055/1	3.31% DW	Airlift glass tubular photobioreactor (8 L)	(Wang et al., 2018)
	TAG	UTEX 640	58.5 mg L ⁻¹ day ⁻¹ 45% DW	Outdoor green wall panel III (≤40 L)	(Butler et al., 2022)
Carbohydrates	Chrysolaminarin	CAS	94 mg L ⁻¹ day ⁻¹ 14% DW	Indoor flat-plate (50 L)	(Rodolfi et al., 2017)
Pigments	Fucoxanthin	CAS	4.7 mg L ⁻¹ day ⁻¹ 0.7% DW	Indoor flat-plate (50 L)	(Gao et al., 2017)
		CCAP 1055/1	1.33% DW	Airlift glass tubular photobioreactor (8 L)	(Gao et al., 2017)

303

304 **Table 2.** Productivity of different target products from *P. tricornutum* strains in
305 phototrophic cultures.

306

307 **2.1.1 Influence of culture parameters on lipids production and composition**

308 The content of bioactive molecules in microalgae can be remarkably affected by the
309 culture conditions and the biochemical composition of biomass is subjected to
310 fluctuations during the culture period. Qiao et. al (2016) performed phototrophic
311 laboratory cultures of *P. tricornutum* Bohlin, from the Microalgae Culture
312 Center (MACC), Ocean University of China, in f/2 medium in 500 mL flasks, irradiated
313 by LED lamps working on a 14:10 h light:dark photoperiod and shaken at 100 rpm. The
314 authors studied the effect of the variation in salinity (15; 20; 28; and 35 ppt), nitrogen
315 concentration (1.24; 12.35; 24.70; and 49.40 mg L⁻¹), light intensity (photosynthetic
316 photon flux density PPF) (50, 100 and 150 $\mu\text{mol m}^{-2} \text{s}^{-1}$ with 14:10 h light:dark
317 photoperiod) and temperature (15; 20; 25°C) over fatty acid composition. Under N-
318 limitation conditions, *P. tricornutum* produced greatly MUFAs and saturated fatty acids
319 at the expenses of PUFAs. However, this nutrient starvation also led to a significant
320 decrease in biomass concentration. The lowest salinity caused the lowest total FAs
321 production, but no variation in FAs composition was observed as a function of salinity.
322 DHA accumulation was increased by rising irradiance, while DHA, EPA, and PUFAs
323 decreased with increasing temperature. N-starvation, low salinity, and low temperature
324 promoted the production of DHA at the expense of EPA. Ultimately, the best biomass
325 productivity was achieved for 28 ppt of salinity, 12.35 mg L⁻¹ concentration of nitrogen,
326 50 $\mu\text{mol m}^{-2} \text{s}^{-1}$ light intensity, and 20°C (Qiao et al., 2016).

327 Even if nitrogen limitation can improve lipid contents in microalgae, higher biomass
328 productivity can be reached in higher nitrogen concentrations; an optimum of 32.09
329 mg/L NaNO₃ was found to be most favorable for algal biomass productivity (Yodsuwan
330 et al., 2017).

331 An indoor flat-plate photobioreactor (50 L) was used to test and study the biochemical
332 composition of *P. tricornutum* obtained from the Institute of Oceanography, Chinese
333 Academy of Sciences. Two different nitrogen concentrations were assayed: 14.5 mmol
334 L⁻¹ (HN) and 2.9 mmol L⁻¹ (LN) of KNO₃. Continuous illumination provided by cool
335 white fluorescent lamps at an irradiance of 300 μmol m⁻² s⁻¹, 25 ± 1°C and air
336 bubbling (enriched with 1% of CO₂) were the operative conditions for the 12 days of
337 growing. The maximum biomass concentration was obtained under HN amounting to
338 4.05 g L⁻¹. However, lipid accumulation was accelerated under the LN condition,
339 which achieved 42.48% DW of total lipids (TLs), compared to 36.69% in HN.
340 Regarding the lipids profile, at first, glycolipids were the components more abundant of
341 TLs under both HN and LN. Neutral lipids, mainly TAGs, increased as culture time
342 proceeded and amounted to 63.84% and 75.7% of TLs in HN and LN conditions. It was
343 also noted that as the growth period was protracted, the proportion of PUFAs
344 experienced a decrease, while saturated fatty acids increased.
345 Arachidonic acid (C20:4), EPA (C20:5), oleic acid (C18:1), linoleic acid (C18:2),
346 palmitic acid (C16:0), palmitoleic acid (C16:1), and myristic acid (C14:0) were the fatty
347 acids detected in most abundance. C16:1 increased from 15.55% to 38.67% of total
348 fatty acids in HN treatment and from 15.40% to 40.96% in LN. C20:5 content
349 drastically declined with culture time (Gao et al., 2017).
350 Besides medium composition, important design considerations for the cultivation
351 system should be accounted for. For example, when designing a photobioreactor
352 system, a parameter to be considered as influencing growth performances is the Gas-
353 Liquid Ratio (GLR). A certain value of gas-liquid ratio can assure the proper culture
354 mix, thus preventing sedimentation, increasing the mass transfer, facilitating the

355 assimilation of nutrients by the cells, and forcing them to shift from dark to light zone.
356 However, an excessive degree of the GLR may damage cells due to mechanical shear
357 stress and cause the evaporation of the culture medium. *P. triornutum* from the
358 freshwater algae culture collection of the Institute of Hydrobiology in China (FACHB-
359 Collection) was grown testing different GLR values to find the optimum experimental
360 condition. A GLR of 1.5 vvm allowed to reach 0.5 d⁻¹ as specific growth rate and
361 227.09 mg L⁻¹d⁻¹ as biomass productivity, which were the highest values obtained along
362 with the highest lipid productivity of 48.48 mg L⁻¹d⁻¹. (Song et al., 2014).

363 **2.1.2 Influence of culture parameters on fucoxanthin production**

364 Fucoxanthin accumulation in *P. triornutum* was studied as influenced by several
365 experimental factors. In particular, it was found to be decreasing as the culture time was
366 prolonged, and the decline was accelerated by nitrogen deficiency (Gao et al., 2017). In
367 contrast, low light intensities have been found to promote higher production of
368 fucoxanthin. For instance, a light intensity of 100 $\mu\text{mol m}^{-2} \text{s}^{-1}$ on *P. triornutum* (CS-
369 29) supplied by the Australian National Algae Culture Collection (ANACC), cultured in
370 5 L photobioreactors with f/2 medium at 25 ± 3 °C, resulted in a greater specific
371 fucoxanthin concentration ($42.8 \pm 19.5 \text{ mg g}^{-1}$) than at $210 \mu\text{mol m}^{-2} \text{s}^{-1}$ ($9.9 \pm 4.2 \text{ mg}$
372 g^{-1}). This behaviour can be explained by considering that the production of this light-
373 harvesting pigment is boosted when low light conditions are applied. Conversely, as the
374 light intensity increases, fucoxanthin's content decreases on behalf of photoprotective
375 pigments. In addition, the composition of growth medium was examined as affecting
376 the growth and fucoxanthin accumulation, after choosing a working irradiance of 150
377 $\mu\text{mol m}^{-2} \text{s}^{-1}$. For this purpose, besides f/2 standard recipe, two other media were
378 prepared: $10 \times \text{f/2}$, where all nutrients' concentrations were increased by 10-fold, and

379 f/2 with only nitrate concentration increased by 10-fold. Cells cultivated with the first
380 enriched medium resulted in a 2-fold final dry cell weight ($0.59 \pm 0.10 \text{ g L}^{-1}$) compared
381 to standard f/2 medium ($0.29 \pm 0.03 \text{ g L}^{-1}$), but a lower specific growth rate.
382 Fucoxanthin concentration was remarkably increased by the medium with nitrate
383 supplementation reaching the maximum of $59.2 \pm 22.8 \text{ mg g}^{-1}$ dry algae, against $23.2 \pm$
384 7.0 mg g^{-1} produced in f/2 medium and $26.7 \pm 13.1 \text{ mg g}^{-1}$ in $10 \times \text{f/2}$ medium. These
385 results clearly indicate that fucoxanthin accumulation in *P. tricornutum* is promoted by
386 supplementation of nitrate in culture medium, even if further investigations are required
387 to understand the processes by which this happens (McClure et al., 2018). Yet, it is
388 worth emphasizing that cellular growth and fucoxanthin production are not directly
389 related as the best culture conditions do not always lead to the highest fucoxanthin
390 production (Gómez-Loredo et al., 2016).

391 **2.1.3 Influence of culture parameters on carbohydrates production**

392 In all algae species, carbohydrates represent the first photosynthetic product exiting the
393 Calvin–Benson cycle, acting as precursors for all cell components. Initially,
394 carbohydrates' production is significant and then decreases due to their conversion into
395 other metabolites required by cells. The evolution of total carbohydrate and
396 chrysolaminarin contents in *P. tricornutum* was studied by Gao et. al (2017), who
397 concluded that major amounts of carbohydrates are obtained when cells are in their
398 exponential growth phase, rather than in cells entering the stationary phase. Besides, N-
399 deplete conditions have proven to induce a fast accumulation of these metabolites.
400 The maximum carbohydrate and chrysolaminarin amounts, under 14.5 mmol L^{-1} of
401 nitrogen, were 21.2% and 17.1% of DW, respectively (Gao et al., 2017).

402 Carbohydrates' accumulation is favoured also by higher light intensities since their
403 degradation takes place in the dark. This was confirmed also by Chauton et al. (2013)
404 who found that carbohydrate content in *P. tricornutum* (CCMP 2561) increased with
405 prolonged illumination or extended light phase considering that the phase in which they
406 are produced is longer, while the phase associated with carbohydrates consumption
407 (darkness) is reduced. Moreover, carbohydrates concentration was increased in cells
408 grown in N-depletion rather than in P-depletion. (Chauton et al., 2013). The study of
409 daily fluctuation in biomass composition of *P. tricornutum* CCAP 1055/1 performed by
410 Jallet et al. (2016) allowed also to state that carbon dislocation between diverse
411 metabolites varies remarkably during the light: dark cycle. For instance, biomass was
412 found richer in TAGs and carbohydrates at the end of the light phase if compared to its
413 start, while the reverse condition resulted in proteins. These daily trends should be
414 accounted for when selecting the right moment to harvest, extract a specific metabolite,
415 or for measuring daily productivity (Jallet et al., 2016). Similar results were obtained on
416 the same strain by Caballero et al. (2016) who presented an experimental procedure to
417 simultaneously characterize and resolve insoluble, soluble reducing, and soluble
418 nonreducing carbohydrates from *P. tricornutum*, to study the carbon partitioning during
419 nitrogen replete and nitrogen deplete conditions. They confirmed, through
420 compositional and structural analysis, the hypothesis that chrysolaminarin belongs to
421 the soluble nonreducing carbohydrate portion.

422 Moreover, by comparing laminarin and chrysolaminarin structures, they observed that
423 *P. tricornutum*' s chrysolaminarin is smaller and lightly branched. During nitrate
424 starvation, chrysolaminarin was produced to store only 4.9–6.0% of cellular carbon,
425 which is definitively lower if compared to the TAG accumulation amounting to 43–

426 50%. This result led the authors to the conclusion that chrysolaminarin is not the
427 preferred storage product during nitrogen limitation. Ultimately, nutrient replete
428 conditions and high irradiance allowed high accumulation of chrysolaminarin in *P.*
429 *tricornutum*, which occurs at night in a 12:12 light:dark cycle, while its consumption is
430 completed by dawn (Caballero et al., 2016).

431 **2.2 Mixotrophic cultivation of *Phaeodactylum tricornutum***

432 Mixotrophic cultivation mode, occurring when an organic carbon source is supplied
433 concurrently with the use of light, allows benefiting from the main advantages of both
434 phototrophy and heterotrophy. This cultivation procedure can hence lead to high
435 biomass productivity while enriching microalgal biomass with the profitable
436 photosynthesis-related metabolites, which are normally missing in heterotrophic mode
437 (Cerón-García et al., 2013).

438 It is noteworthy that mixotrophy demands proper uptake proteins that enable the
439 metabolism of the chosen carbon source. If their upregulation and expression employ
440 too much time, a lag phase in population growth may result (Penhaul Smith et al.,
441 2020). Nevertheless, compared to phototrophic cultures, growth rates, and biomass
442 production increase thanks to the synergy established between light and the organic
443 source. In mixotrophic cultures, the cellular composition varies according to the period
444 that cells spend in dark and enlightened areas, or, in other words, the respective
445 contribution of the heterotrophic and phototrophic metabolisms to the total growth.
446 In high-density cultures, occurring for high cell concentrations, the light fails to reach
447 efficaciously all cells so that the contribution of the phototrophy to the overall growth
448 rate decreases and the consumption of the organic carbon source becomes sustaining the
449 growth. Even if mixotrophy is a promising alternative culture method to improve

450 biomass productivity, its potential and applicability can vary according to the target
451 metabolite. An optimal balance exists indeed between phototrophic and heterotrophic
452 growth for the optimal productivity of every specific compound (Cerón-García et al.,
453 2013, 2005, 2000). Recent studies tried to unravel the molecular function of mixotrophy
454 by concluding that the optimized photosynthetic efficiency in diatoms is achieved
455 through cooperation between mitochondria and plastids. Actually, the synergic actions
456 of these organelles, through exchanges of ATP and NADH, enable close coordination
457 between respiration and photosynthesis, thus simultaneously improving the uptake of
458 light and organic carbon during mixotrophy (Villanova et al., 2017).

459 Several organic compounds such as glycerol, acetate, glucose, fructose, starch, and
460 glycine can be used to cultivate the model diatom *P. tricornutum*, and some studies
461 tested this capacity through the years. **Table 3** shows maximum biomass productivities
462 and concentrations arising from the use of different organic sources on *P. tricornutum*
463 under mixotrophic conditions. In **Table 4** the maximum productivities of diverse
464 compounds obtained from *P. tricornutum* in mixotrophy conditions are collected.
465

Strain	Organic carbon source	Maximum biomass productivity	Maximum biomass concentration	Reference
UTEX 640	Glucose 5 g L ⁻¹	10.70 mg L ⁻¹ h ⁻¹	2.01 g L ⁻¹	(Cerón-García et al., 2005)
	Acetate 0.05 M	13.2 mg L ⁻¹ h ⁻¹	1.15 g L ⁻¹	
	Glycine 0.01 M	11 mg L ⁻¹ h ⁻¹	2.46 g L ⁻¹	
	Starch 1 g L ⁻¹	11.3 mg L ⁻¹ h ⁻¹	1.79 g L ⁻¹	
	Lactic acid 0.005 M	7.73 mg L ⁻¹ h ⁻¹	2.18 g L ⁻¹	
	Glycerol 0.1 M	17.5 mg L ⁻¹ h ⁻¹	2.99 g L ⁻¹	
CCAP 1055/1	Glycerol 0.05 M	-	11.55 g L ⁻¹	(Cerón-García et al., 2005)
UTEX 640	Fructose 0.02 M	6.8 mg L ⁻¹ h ⁻¹	8.2 g L ⁻¹	(Villanova et al., 2021)
	Glycerol 0.1 M	14 mg L ⁻¹ h ⁻¹	14 g L ⁻¹	

466

467 **Table 3.** Maximum biomass productivity and concentration of *P. tricornutum* on

468 different organic sources under mixotrophic cultures.

469

Product	Strain	Organic carbon source	Product yield / productivity	Reference
EPA			9.51 ± 0.13 mg L ⁻¹ d ⁻¹	
Fucoxanthin	CCAP 1055/1	Glycerol	1.97 ± 0.34 mg L ⁻¹ d ⁻¹	(Butler et al., 2022)
FAMEs			51.96 ± 0.61 mg L ⁻¹ d ⁻¹	
EPA		Glycerol	8.56 mg L ⁻¹ d ⁻¹	
		Glycerol 0.1 M + Urea	11.53 mg L ⁻¹ d ⁻¹	
Total Pigments	UTEX 640	Lactic acid	4.45% DW	(Cerón-García et al., 2005)
Chlorophylls		Lactic acid	3.79% DW	
Carotenoids		Starch	1.04% DW	

470

471 **Table 4.** Productivity of different target products from *P. tricornutum* strains in

472 mixotrophic cultures.

473

474 2.2.1 Glycerol

475 The effect of glycerol on *P. tricornutum* metabolism has been assessed via
476 transcriptomics, metabolomics, metabolic modelling, and physiological studies. Results
477 point out that carbon-storage, central-carbon, and lipid metabolism are all affected by
478 the presence of this compound. In metabolic pathways of *P. tricornutum*, glycerol
479 converts to glycerol phosphate, through the action of glycerol kinase, which constitutes
480 the precursor for TAG synthesis, and to dihydroxyacetone phosphate, through the action
481 of glycerol-3-phosphate dehydrogenase, in the glycolysis and pentose phosphate
482 pathway (PPP), thus influencing the central-carbon metabolism. In the case of
483 phototrophy, the diatom's carbon requirement is instead satisfied by the consumption of
484 the inorganic carbon source occurring in the Calvin cycle, characterized by higher
485 enzymatic and light energy costs. The supply of glycerol simulates the characteristic
486 effects of N-starvation on lipid production, contributing to the triacylglycerol and fatty
487 acid accumulation. Nevertheless, unlike nitrogen-deplete conditions which affect
488 biomass productivity, the presence of glycerol neither decreases photosynthetic ability
489 nor diatom's growth (Villanova et al., 2021, 2017).

490 Cerón-García et al. (2000) reported the EPA production from *P. tricornutum* UTEX 640
491 strain under mixotrophic conditions using glycerol and studied the effect of different
492 glycerol concentrations (0.005; 0.01; 0.05; and 0.1 M) and subsequent additions of
493 glycerol and ammonium chloride on growth kinetics, biomass productivity, and fatty
494 acid profiles. The authors used one-liter flasks with enriched seawater medium that
495 were sparged with filter-sterilized air (0.22µm Millipore filter) at 0.1 v/v min⁻¹ to mix
496 the suspension. The cultures were continuously illuminated at an irradiance of 165 µmol
497 photons m⁻² s⁻¹ at a temperature of 20 ± 0.5°C. The optimal initial concentration of

498 glycerol was determined as 0.1 M, which resulted in maximum biomass productivity
499 and concentration of $17.5 \text{ mg L}^{-1} \text{ h}^{-1}$ and 2.4 g L^{-1} , respectively. However, a lag phase
500 lasting for the first 160 h of growth was observed for cultures grown with higher
501 glycerol concentrations; they indeed maintained a biomass concentration below that of
502 the control (in absence of glycerol). No lag phases were observed for lower glycerol
503 concentrations, which indicates that this physiological response was due to an
504 adaptation period to a high glycerol environment. Once the optimal glycerol
505 concentration was established, a fed-batch culture was performed by operating
506 sequential additions of ammonium chloride and glycerol. In these conditions, the
507 resultant EPA productivity equal to $33.5 \text{ mg L}^{-1} \text{ d}^{-1}$ was recorded as the highest
508 obtained (Cerón-García et al., 2000).

509 In another study, different pilot-scale photobioreactors systems were used for the
510 cultivation of *P. tricornutum* UTEX 640 strain, grown in fed-batch and under
511 mixotrophic conditions: outdoor vertical bubble column (BC), draft-tube airlift (DT),
512 and split-cylinder (SC), each of 60 L working volume. The diatom was grown on a
513 modified Ukele medium supplemented with an initial 0.1 M of glycerol, with
514 subsequent additions of nutrients (glycerol, ammonium, urea), which instantaneously
515 improved the growth rate. Best performance in terms of maximum biomass
516 concentration was reached in SC photobioreactor with 25.4 g L^{-1} . The supplied organic
517 nutrient did not significantly affect carotenoids and chlorophylls content since they
518 remained at 0.4-0.8% and 1.5-2.0% DW respectively. EPA content raised to 3% DW
519 reaching a productivity of $56 \text{ mg L}^{-1} \text{ d}^{-1}$ (Fernández Sevilla et al., 2004).

520 Furthermore, *P. tricornutum* (CCAP 1055/3 axenic strain) was cultivated in a 250 mL
521 Erlenmeyer using an artificial seawater medium enriched with extra nitrogen and

522 phosphorus (ESAW) to obtain 0.47 g L⁻¹ N and 0.03 g L⁻¹ P. Cultures were conducted
523 in phototrophy with N-depletion (PHOT-N) shaken at 100 rpm and 20°C, under a light
524 intensity of 40 μE m⁻² s⁻¹ with a 12h:12h light:dark cycle. Regarding mixotrophic tests,
525 glycerol was supplemented to the medium to reach a final concentration of 50 mM in
526 both N-replete and N-deplete tests. Glycerol enhanced biomass production by 2-fold
527 compared to growth in PHOT medium, favoring nitrogen and phosphate consumption,
528 and did not inhibit the photosynthetic ability. Moreover, its presence affected cellular
529 lipid content by increasing TAG accumulation in both nitrogen-replete and starved
530 cells. These results suggest that glycerol act as TAG-booster by providing the glycerol
531 backbone and the acyl groups required for TAG assembly (Villanova et al., 2017).
532 In a follow-up study, the optimized ESAW medium (added with sodium bicarbonate
533 and extra nitrogen and phosphorous) was used to grow *P. tricornutum* (CCAP 1055/3
534 strain) in mixotrophy with glycerol (4.6 g L⁻¹) in a 2 L photobioreactor sparged
535 continuously with air at a flow rate of 0.5 L min⁻¹ and under a controlled temperature
536 of 20°C. Cultures were continuously illuminated by a variable light intensity of 70 to
537 300 μmol m⁻² s⁻¹. These fluorescence studies were conducted to determine the light
538 dependency of NPQ: a value of 400 μE was found as sufficient to obtain the maximum
539 value of fluorescence, without provoking damage to the photosynthetic system. The
540 biomass concentration was found to increase by a factor of 9 in the optimized medium
541 compared to the conventional enriched seawater medium. Moreover, both biomass
542 quantity and quality were enhanced by the provision of the organic and inorganic
543 (NaHCO₃) carbon sources. Both respiration and photosynthesis performances were
544 improved in these mixotrophic tests, confirming the energetic coupling of these two

545 metabolic processes. Ultimately, the optimized medium allowed to obtain higher
546 productivity in biomass and lipids compared to other studies (Villanova et al., 2021).

547 **2.2.2 Other carbon sources**

548 Other carbon sources tested on *P. tricornutum* under mixotrophic conditions are acetate,
549 glucose, fructose, starch, glycine, and lactic acid. Acetic acid is metabolized bonded to
550 acetyl-CoA protein and carried in the glyoxysome, by entering the TCA cycle
551 (tricarboxylic acid cycle) in the mitochondria, or directly used for fatty acid
552 biosynthesis, which provides an increase in respiration and carbohydrate accumulation
553 (Penhaul Smith et al., 2020).

554 *P. tricornutum* UTEX-640 strain growth was tested on different substrates at diverse
555 concentrations in fed-batch and discontinuous modes (fed-batch only for glycerol). The
556 nutrients assayed were glucose (0.5 to 5 g L⁻¹), acetate (0.005 to 0.1 M), glycerol (0.005
557 to 0.1 M), lactic acid (0.005 to 0.1 M), starch (0.5 to 5 g L⁻¹), glycine (0.005 to 0.02
558 M). Filter-sterilized air at 0.1 vvm was used to mix and aerate the cultures. These were
559 constantly irradiated at 165 μmol m⁻² s⁻¹ and maintained at 20 ± 0.5°C. The authors
560 studied biomass productivity and biochemical composition. Experiments with acetate
561 indicated that growth inhibition occurs above 5 mM: growth was decelerated, and
562 biomass concentration and productivity declined. Contrastingly, growth was stimulated
563 by all starch concentrations tested, and only a slight inhibitory response was reported
564 for concentrations above 2 g L⁻¹ of starch. Lactate consistently promoted growth in
565 most experiments, gaining the maximum biomass concentration for 5 mM; however, a
566 possible inhibition was detected for 0.1 M of lactate which induced the decrease of final
567 biomass concentration. All concentrations of glucose resulted in a stimulating effect for
568 the growth, although not very intense. The study of the organic substrate as influencing

569 metabolites production led to varied results. If lactate, glycine, glycerol, and starch
570 stimulated the biosynthesis of total pigments on one side, an opposite effect was
571 observed for glucose. Same trends were found for chlorophyll contents. EPA
572 productivity was remarkably influenced by nutrient source: lactate and glucose
573 increased EPA content, while starch decreased it. Glycine had no significant influence
574 on cellular EPA concentration (Cerón-García et al., 2005). Another study compared the
575 mixotrophic cultivation of *P. tricornutum* UTEX-640 strain grown on fructose and
576 glycerol. These cultures were performed in bubble photobioreactors (2 L) in fed-batch
577 mode, with enriched seawater as medium, temperature maintained at $20 \pm 0.5^\circ\text{C}$, use of
578 CO_2 for pH control, and a sparging air flow rate of 1.5 vvm. Diverse nutrient-supply
579 procedures, along with a sequential increase of irradiance (280 to $750 \mu\text{E m}^{-2} \text{s}^{-1}$) were
580 assayed. At first, the batch mode was employed to initiate the cultures; then, when cells
581 enter the stationary stage, the nutrient supply and/or irradiance increment was executed.
582 During the first part of the cultivation (117 h), the biomass concentration raised
583 similarly to phototrophic control, and no fructose was consumed, indicating that high
584 percentages of inorganic carbon (CO_2 and HCO_3^-) can force the diatom to grow
585 phototrophically, which, in turn, inhibits the assimilation of organic carbon. The
586 consumption of fructose was initiated when the CO_2 injection for pH monitoring was
587 discontinued; consequently, cell growth and biomass concentrations immediately raised
588 upon the organic C source consumption. Despite this, final biomass concentrations of
589 mixotrophic cultures with fructose were lower than the phototrophic control (Cerón-
590 García et al., 2013).

591 **2.2.3 Waste effluents**

592 Recently, industrial, agricultural, and municipal wastewater effluents have been
593 efficaciously tested for microalgae cultivation and production. There is no lack of
594 studies testing the growth performances of *P. tricornutum* by adding wastewater
595 effluents to the culture medium. The recovery of nutrients contained in these types of
596 effluents can reduce the cost of fertilizers and has the advantage of reducing the amount
597 of nutrient-rich digestate to dispose of, while eventually lowering the costs associated
598 with microalgae cultivation thus promoting a circular economy approach (McDowell et
599 al., 2020; Su et al., 2020). *P. tricornutum* batch cultures were grown mixotrophically
600 with glycerol as carbon source and ultrafiltered digestate (UF) from a biogas plant as
601 nitrogen source, testing different concentrations of glycerol (0.02; 0.03; 0.04 M). In
602 their study, the strain SAG1090-1a was cultivated in a 0.5 L photobioreactor at 25°C, at
603 a constant air flux of 10 L min⁻¹, 312 μmol m⁻² s⁻¹, and a 12h:12h photoperiod. CO₂
604 injection was used to control pH at 8 and the f/2 culture medium was added with UF
605 and different concentrations of glycerol. The highest biomass concentration reached was
606 4.96 g L⁻¹ corresponding to an addition of 0.04 M of glycerol. Biomass productivity
607 increased by 1.29 and 1.60 times, compared to the control, with 0.03 M and 0.04 M of
608 glycerol respectively. The balance study performed on nitrogen demonstrated that UF
609 supplement increased nitrogen availability, thus promoting algal growth and protein
610 accumulation. Regarding diatom's biochemical properties, the highest glycerol
611 concentrations caused a decline in protein content due to N limitations, while lipid
612 content did not show variability as UF and/or glycerol were provided. However, the
613 fatty acid profile changed compared to the phototrophic control: under mixotrophic
614 conditions, saturated fraction increased at the expense of ω-3 and PUFAs contents. The
615 supply of glycerol was found to switch the metabolism to carbohydrate production,

616 whose content displayed a remarkable increase. Nevertheless, the authors reported that
617 carbohydrates' increase and proteins' decrease were also a consequence of nitrogen
618 starvation induced by microbial competition, which forced the diatom towards
619 carbohydrates accumulation (Su et al., 2020).

620 Anaerobic digestate also represents a rich source of nitrate, ammonium, phosphorous,
621 and trace micronutrients required for microalgae growth, although high concentrations
622 of ammonium ($> 80\text{-}100 \text{ mg L}^{-1}$) can potentially inhibit it. Three AD plants were
623 selected to investigate how their effluents affect the biochemical profile of *P.*
624 *tricornutum*: (1) cow slurry and grass silage (CW); (2) pre-consumer food waste (FW);
625 (3) pig slurry and grass silage (PW). 5 L photobioreactors irradiated by $170 \mu\text{mol m}^{-2}$
626 s^{-1} at $20 \pm 1 \text{ }^\circ\text{C}$, were used for the trials. *P. tricornutum* CCAP 1052/1B strain was
627 cultivated in digestate media of different concentrations obtained by supplementing 1%,
628 3%, or 6% v/v liquid digestate stream to seawater. All these media provided enough
629 nourishment for *P. tricornutum* cells, whose growth rate was similar or higher to the
630 ones reached in the f/2 control. Initial lag phases of cell adaptation were observed for
631 higher concentrations of effluent. All concentrations of CW and FW resulted in a
632 considerable enhancement of crude protein production compared to the control. CW 1%
633 produced microalgae richer in $\omega\text{-}3$ and EPA, compared to PW 1%, but similar to
634 control. Major quantities of fatty acids DW were obtained in microalgae grown in lower
635 levels of digestate concentrations, being CW 1% and PW 1% the ones to produce the
636 highest values of total fatty acids. Ultimately, CW 1% digestate has proved to be the
637 best digestate in terms of the total fatty acids and proteins accumulation (McDowell et
638 al., 2020).

639 The suitability of this diatom to grow also in municipal wastewater (MW) mixed with
640 seawater (SW) in compositions MW:SW = 1:1 and MW:SW = 2:1 was tested
641 successfully. *P. tricornutum* CCMP632 strain was grown at 18 °C and 120 $\mu\text{mol m}^{-2} \text{s}^{-1}$
642 under a 12h:12h photoperiod. The final biomass increased by about 40% compared to
643 f/2 control, indicating the possibility of using this type of effluents to grow the species.
644 Growth performances were further enhanced in cultures supplemented with air aeration,
645 which also facilitated lipids accumulation. MW: SW=1:1 and f/2 medium tests allowed
646 to obtain the highest quantities of lipid (34.4% and 35.5%); furthermore, MW: SW=1:1
647 condition accomplished also the highest lipid productivity (33.20 $\text{mg L}^{-1} \text{day}^{-1}$) (Wang
648 et al., 2019). Besides the employment of wastewater effluents, the recycling of CO₂ flue
649 gases for growing microalgae represents a further step towards the exploitation of waste
650 resources in a circular economy perspective. Simonazzi et al. (2019) evaluated the
651 viability of employing both waste CO₂ and a pre-treated digestate to cultivate *P.*
652 *tricornutum* and optimize growth and ω -3 productivity in the successive scale-up.
653 Biomass productivity and accumulation of PUFAs were not altered when using waste
654 CO₂. *P. tricornutum* growth was resulted completely supported by the pre-treated
655 digestate and waste CO₂, without the risk of inhibition, to a final biomass density of 1-
656 1.2 g L^{-1} . The biochemical composition of resulted biomass after 15 days of culture
657 was: proteins 36-37%, lipids 34-35%, and polysaccharides 5-6%. The authors reported
658 no differences between biomass grown with flue gas and biomass grown with pure CO₂.
659 (Simonazzi et al., 2019).
660 Other research has also proved the opportunity of growing diverse microalgae species
661 on such effluents, thus potentially reducing the high costs necessary to sustain their
662 industrial production, in terms of nutrient needs (representing 30–40% of operating

663 costs). At the same time, this solution would allow to purify wastewater effluents and
664 eventually dispose of CO₂ off-gas thus also promoting climate change mitigation,
665 through an economic and environmentally friendly approach. This would be
666 advantageous also for saving money required to recycle and depurate waste streams by
667 removing nutrients (Wang et al., 2019). However, it should be underlined that the
668 chemical profile and complex composition of the effluent will strongly influence the
669 resultant biochemical composition of microalgal biomass, thus influencing its
670 downstream valorisation pathway and possible applications (McDowell et al., 2020).
671 Moreover, with regards to CO₂ streams, the presence of the typical substances
672 constituting flue gases such as NO_x, SO_x, and heavy metals, should be controlled due
673 to the possibility of culture medium acidification, harmful to the cells, and the
674 bioaccumulation of toxic compounds in the resulting biomass, which eventually
675 compromises its quality and subsequent applicability (Simonazzi et al., 2019).

676 **3. Extraction of value-added products from *Phaeodactylum tricornutum***

677 Among microalgae species, diatoms are indicated as an auspicious feedstock for the
678 biotechnology sector, since multi-product and fractionation procedures would be able to
679 launch new production chains in different industrial fields (Savio et al., 2020). Although
680 the products recoverable from microalgae are highly profitable from an economic
681 perspective, their industrialization still struggles to establish on the market. Among the
682 reasons, high investments required for downstream purification steps contribute
683 significantly. Moreover, these conventional processes making use of a huge quantity of
684 organic solvents, produce a heavy impact on the environment. Lipid fraction from
685 microalgal biomass has been usually extracted by employing toxic solvents such as
686 chloroform, n-hexane, diethyl ether, methanol, and their mixtures. Therefore, extensive

687 studies have been conducted on the optimization of extraction technologies and
688 especially on the design of new protocols excluding the use of toxic solvents to increase
689 efficiency and sustainability, reduce waste production, and decrease energy
690 consumption. Some green extraction techniques complying with these requirements are
691 Supercritical Fluid Extraction (SFE), Pressurized Liquid Extraction (PLE), Ultrasound-
692 Assisted Extraction (UAE), Microwave-Assisted Extraction (MAE), Pulsed Electric
693 Field (PEF), Enzymatic-Assisted extraction (EAE), and alternative solvents like deep
694 eutectic solvents (DES), and ionic liquids (ILs). Briefly, UAE and MAE make use of
695 generally recognized as safe solvents (GRAS) such as water and ethanol, while
696 enhancing and boosting their extractive capacity, also reducing operating temperature,
697 extraction time, and solvent consumption. During ultrasonication, high-frequency
698 acoustic waves cause a cavitation effect, which culminates in the cell disruption by high
699 shear forces. MAE instead consists in transferring energy to the solution, through the
700 concurrence of dipole rotation and ionic conduction mechanisms. Polar molecules, such
701 as the water inside the cells, absorb the energy and heat up rapidly causing the pressure
702 inside the cell to increase till the cell ruptures and releases cell compounds (Günerken et
703 al., 2015; Zhou et al., 2019). SFE employs a determinate solvent (such as CO₂) at
704 pressures and temperatures higher than the critical point (31.2 °C and 73.8 bar for CO₂)
705 that improve its solvent capacity. This technology also offers the possibility to use a co-
706 solvent to modify the overall polarity and selectively extract specific compounds. PLE
707 applies high temperature (but lower than the critical point) and pressures sufficiently
708 high to keep the solvent liquid. In this case, the solvent possesses augmented solubility
709 and lower viscosity which in turn improves mass transfer and permeation into the
710 biomass sample (Gallego et al., 2018). During PEF, an electrical potential throughout

711 the cell wall is originated by the application of an external electric field. In this case,
712 cell disruption is accomplished by electromechanical compression (Günerken et al.,
713 2015). In addition, ionic liquids are emerging as an interesting alternative to fractionate
714 microalgal biomass. These are low melting salts that are generally used to perform soft
715 and selective extractions from both non-disrupted and disrupted biomass while
716 preserving structural integrity and bioactivity of metabolites (Eppink et al., 2021). The
717 extraction of fucoxanthin from *P. tricornutum* biomass (provided by
718 the Microalgae Collection of Ningbo University) was carried out to investigate the
719 effects of a few factors on fucoxanthin's yield. These factors were the solvent used
720 (methanol, ethanol, acetone, water, and ethyl acetate, ethanol-water mixtures from 60%
721 to 100 % v/v), extraction time (15 to 120 min), extraction temperature (4 to 40 °C), and
722 total extraction rounds. The decreasing order of the solvent's performance in terms of
723 fucoxanthin extraction yield was the following: 1) methanol; 2) ethanol; 3) acetone and
724 ethyl acetate. Thereby, better extraction performances were accomplished when using
725 polar solvents. Even if methanol was revealed to be the most efficient for extracting
726 fucoxanthin, also the greener mixture of 70% ethanol-water performed well. The
727 quantity of fucoxanthin extracted was favored by the increase in operating time and
728 temperature. Moreover, the first extraction was enough to obtain about 80% of the total
729 fucoxanthin. Hence, the optimum experimental conditions to mildly extract fucoxanthin
730 from *P. tricornutum* biomass were solvent/solid ratio equal to 40 mL g⁻¹, operating time
731 90 min, 25°C, 70% mixture ethanol-water, and one extraction round. These
732 conditions allowed to have an extract containing both lipids and fucoxanthin. Therefore,
733 this extract was further purified by an ethanol precipitation process at 25°C, which led
734 to an extraction yield of 7.14 ± 0.11 mg g⁻¹ with a recovery percentage of 80.04 ±

735 1.18%. (Sun et al., 2022). Gilbert-López et al. performed a comparison between MAE
736 and PLE technologies for extracting value-added compounds from *P.*
737 *tricornutum* freeze-dried biomass provided by Fitoplancton Marino S.L. and studied the
738 effects of temperature, solvent, and extraction time. A factorial Design of Experiment
739 (DoE) sized 3^2 was conducted to investigate PLE performance and optimize
740 experimental conditions. The investigated factors were temperature (50; 110; 170 °C)
741 and ethanol in different percentages (0; 50; 100%). Whereas the 3^3 factorial design for
742 MAE studied the following factors: extraction time (2; 11; 20 min), composition of
743 ethanol (0; 50; 100%), and temperature (30; 100; 170 °C). The response variables for
744 both DoE studies were extraction yield, antioxidant activity (indicated as Trolox
745 equivalent antioxidant capacity TEAC), total carotenoids, chlorophylls, and total
746 phenols content (TPC). For PLE, the temperature was found to have a positive effect on
747 extraction yield, indicating that it improved the mass transfer, and the solvent solubility,
748 while reducing its viscosity, thus promoting the solvent permeation ability. The solvent
749 mixture water-ethanol (50:50) reached higher yields, compared to pure solvents.
750 Whereas higher phenols content and antioxidant activity were found for pure
751 ethanol. The content of carotenoids increased with a higher percentage of ethanol and
752 decreased with the temperature. Regarding MAE process, the extraction time did not
753 show any significant effect on all response variables. Like PLE, the temperature had a
754 favorable influence on extraction yield also in MAE, and the same was observed when
755 water was present in the solvent mixture; the lowest yields were indeed obtained with
756 pure ethanol. Higher phenolic and TEAC content were found in pure ethanol. Finally,
757 carotenoids were primarily extracted by 100% ethanol, but their content decreased with
758 the temperature, indicating the possibility of compound degradation. Optimum

759 extraction conditions for PLE and MAE were modeled to maximize each response
760 variable, all response variables, and all variables except the yield (**Table 5**). HPLC–
761 APCI–MS/MS was used to characterize the extracts obtained at optimum conditions.
762 Fucoxanthin was the most abundant compound; then diatoxanthin, other two
763 carotenoids, and one carotenoid ester were detected. Other minor peaks in the
764 chromatogram were attributed to chlorophylls, having the same absorbance
765 spectrum. The amount of fucoxanthin recovered in PLE and MAE is also presented in
766 **Table 5**. MAE optimum extracts were richer in phenols, carotenoids, and TEAC;
767 however, higher extraction yields were obtained from PLE. Regarding fucoxanthin, its
768 concentration was similar between MAE and PLE extracts, but its recovery was better
769 with PLE technology thanks to the higher extraction yield (Gilbert-López et al., 2017).
770

771

Optimum modeled extraction conditions	PLE	MAE	Recovered fucoxanthin [mg g ⁻¹ algae]
Yield maximization	170 °C; 40% EtOH	170 °C; pure water; 20 min	-
TPC maximization	50 °C; 100% EtOH	30 °C; 100% EtOH; 2 min	7.73 (PLE)
TEAC maximization	50 °C; 100% EtOH	170 °C; 100% EtOH; 2 min	
Carotenoids maximization	170 °C; 100% EtOH	30 °C; 100% EtOH; 2 min	-
Yield, TPC, TEAC, and carotenoids maximization	170 °C; 97% EtOH	170 °C; 100% EtOH; 5.8 min	5.81 (PLE), 2.97 (MAE)
TPC, TEAC and carotenoids maximization	50 °C; 100% EtOH	30 °C; 100% EtOH; 2min	4.59 (MAE)

772

773 **Table 5.** Modeled optimum conditions for extraction of valuable compounds from *P.*774 *tricornutum* using PLE and MAE.

775

776 Tommasi et al. (2017) also explored the lipid extraction from *P. tricornutum* (furnished
777 by Micoperi Blue Growth) by using dimethyl carbonate (DMC) solvent extraction (a
778 nonvolatile, cheap, non-corrosive, non-toxic, and eco-friendly solvent) and supercritical
779 CO₂ (scCO₂). Microwaves (MWs) and deep eutectic solvents (DESs) and their
780 combination were used as pretreatments for both extractions and their performances
781 were evaluated. The authors tested the application of different DESs obtained by
782 choline chloride and diverse hydrogen donors, concluding that DESs obtained by ChCl
783 and carboxylic acids was the best solvent among the tested ones, as higher selectivity
784 and an enhancement of total fatty acid (TFA) extraction performances of DMC were
785 determined. Instead, the MW process alone did not enhance DMC extraction capacity,
786 which remained scarcely effective or selective. The combination of DESs and MW
787 pretreatments and the subsequent DMC extraction resulted in a TFA yield and fatty acid
788 profile similar to those obtained by the conventional Bligh and Dyer procedure, together
789 with a much-improved selectivity (88% against 35%). The combination DES-MW
790 remarkably enhanced the extraction efficiency of scCO₂, improving the TFA yield by
791 20-fold and obtaining very purified extracts. Despite DES-scCO₂ extracting lower
792 quantities of total fatty acids than DES-MW-scCO₂, it resulted in the highest content of
793 EPA (35%). Neither DES nor DES-MW pretreatments were found to degrade PUFAs
794 and EPA, which hence can be effectively extracted employing DMC and scCO₂
795 procedures (Tommasi et al., 2017). No other extraction technologies have been
796 proposed and tested for *P. tricornutum* so far, except for some studies concerning the
797 combined production of diverse value-added compounds in a biorefinery approach that
798 will be discussed in the next section. Hence, other, especially environmentally friendly
799 techniques should be assessed on this interesting diatom both to identify the best

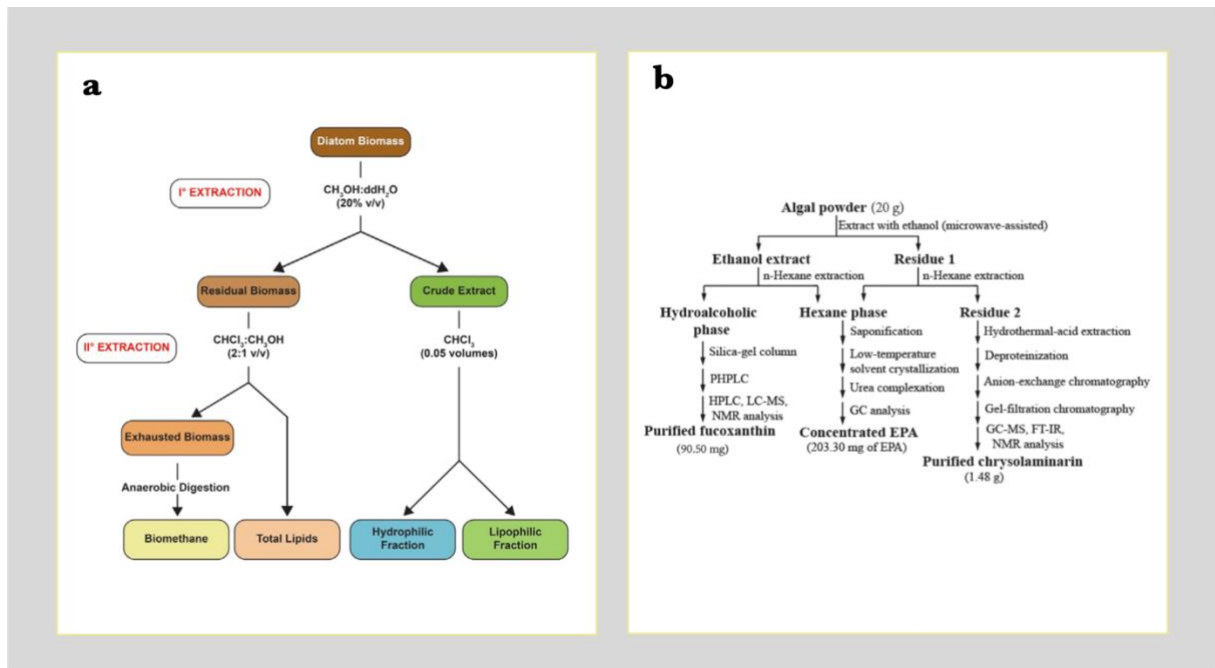
800 extraction conditions leading to the highest yields and to determine what is extracted
801 and what remains in the residual if it is undamaged, thus exploring the possibility of a
802 cascade extraction and purification of algae biomass.

803 **3.1 Biorefinery approaches**

804 Currently, at a commercial scale, just a single compound (e.g., astaxanthin, β -carotene)
805 is produced from microalgae sources, while other conceivably fractions such as proteins
806 and carbohydrates, are disposed of. Instead, to enhance the economic feasibility of
807 bioactive compounds production from microalgae, all biomass fractions should be
808 valorised, leading to a multi-product biorefinery (Bhattacharya and Goswami, 2020;
809 Branco-Vieira et al., 2020). A microalgae-based biorefinery would then rely on an
810 industrial chain producing microalgal biomass under optimal conditions and,
811 subsequently, a facility generating a broad range of products, such as chemicals, food
812 additives, health-enhancing compounds, and biofuels, exactly as occurs for petroleum-
813 based processes (Gilbert-López et al., 2015). Some studies developed and tested
814 cascade extractions on *P. tricornutum* to obtain multiple compounds production in a
815 perspective of biorefinery. For example, a multi-step aqueous and non-aqueous
816 extraction was developed for *P. tricornutum* biomass provided by Algosource Saint-
817 Nazaire, as follows: high voltage electrical discharges (HVED: 1-8 ms; 40 kV cm⁻¹) or
818 high-pressure homogenization (HPH: 10 passes; 1200 bar) (first step); aqueous
819 extraction to obtain carbohydrates, proteins, and water-soluble pigments (second step);
820 liposoluble pigments extraction by 95% ethanol (third step); and lipids extraction by
821 chloroform and methanol (fourth step). Characterizations of proteins, carbohydrates,
822 ionic compounds, and hydro-soluble pigments were conducted to test the extraction
823 performances of the two pre-treatments employed. The authors showed how HVED

824 performed better selective extraction of hydro-soluble compounds. However, the
825 efficiency of HPH treatment in disrupting microalgal cells and extracting hydro-soluble
826 compounds (carbohydrates and proteins) was higher; while the non-aqueous extraction
827 (third and fourth steps) of pigments and lipids was more efficient when HVED was
828 used. Overall, the pre-treatments allowed to improve the amounts of components of
829 interest in the extracts, compared to the untreated samples (Zhang et al., 2020). **Figure**
830 **2a** shows another stepwise extraction procedure to produce multiple-valued compounds
831 from the same biomass of *P. tricornutum*, used as lyophilized biomass from
832 Phytobloom Necton. A crude extract was first obtained using methanol (20% v/v);
833 successively, chloroform and methanol (2:1 v/v) were adopted to obtain total lipids
834 from the remaining biomass, and finally, the “leftover” material, was subjected to
835 anaerobic digestion to assess its Biochemical Methane Potential (BMP). The crude
836 extract obtained from the first step was further separated into a hydrophilic fraction and
837 a lipophilic one by adding 0.05 volumes of chloroform. Obtained fractions from the
838 extraction protocol were then characterized using NMR analysis, bioactivity test, and
839 fatty acid profile analysis. The lipid content of the residue from step 2 was 17.09% ±
840 1.50%. Final exhausted biomass provided an Organic Fraction content of 88.07 ± 0.50%
841 and led to 164.8 ± 10.3 ml g⁻¹ of organic fraction as methane yield (Savio et al., 2020).
842 Another study proposed a stepwise extraction process on *P. tricornutum* to obtain EPA,
843 chrysolaminarin, and fucoxanthin in a biorefinery concept, utilizing different solvent
844 solutions (**Figure 2b**). The algal powder was first subjected to a Microwave-Assisted
845 Extraction with ethanol; then both extract and residue were treated with hexane and
846 resulted in three fractions: hydroalcoholic phase, which was further purified to obtain
847 fucoxanthin, hexane phase, which gave a concentrate in EPA after few other steps, and

848 a residue, from which chrysolaminarin was separated. The yields obtained were $34.03 \pm$
 849 0.72% , $23.00 \pm 0.29\%$, and $43.54 \pm 0.91\%$ DW, respectively. Moreover, the use of
 850 ethanol and MW treatments of 1 min resulted in the highest fucoxanthin yield (Zhang et
 851 al., 2018). Although these works are the first reports on the comprehensive utilization of
 852 *P. tricornutum* biomass, the use of toxic solvents was still selected. Moreover, as
 853 depicted in **Figure 2b**, the developed step-wise extraction is composed of numerous
 854 steps, which could be hardly scaled up at the industrial level. Hence, it should be further
 855 explored the possibility of designing a biorefinery based on *P. tricornutum* biomass
 856 making ideal use of exclusively green extraction technologies and safe solvents.



857
 858 **Figure 2.** Step-wise extraction of value-added compounds from *P. tricornutum* biomass
 859 in a biorefinery perspective. **a)** (Savio et al., 2020) **b)** (Zhang et al., 2018)

860

861 **4. Conclusions**

862 As illustrated, *Phaeodactylum tricornutum* shows great potential in the microalgae
863 sector to produce valuable compounds. Glycerol was confirmed as the best organic
864 source for growing this diatom mixotrophically, enhancing both biomass concentration
865 and growth rate. Beyond EPA, fucoxanthin, and chrysolaminarin, other valuable
866 compounds worth to be studied could be present in extraction biomass residuals.
867 Therefore, more effort should be addressed to the study of green extraction methods in a
868 biorefinery concept, also exploring the possibility of using wet extraction methods thus
869 saving the energy required for the drying step. Finally, techno-economic analysis and
870 Life Cycle Assessment could be used to assess the effective potential of a microalgae-
871 biorefinery.

872 **5. Acknowledgments**

873 This research did not receive any specific grant from funding agencies in the public,
874 commercial, or not-for-profit sectors.

875 **6. References**

- 876 1. Araújo, R., Vázquez Calderón, F., Sánchez López, J., Azevedo, I.C., Bruhn, A.,
877 Fluch, S., Garcia Tasende, M., Ghaderiardakani, F., Ilmjärv, T., Laurans, M.,
878 Mac Monagail, M., Mangini, S., Peteiro, C., Rebours, C., Stefansson, T.,
879 Ullmann, J., 2021. Current Status of the Algae Production Industry in Europe:
880 An Emerging Sector of the Blue Bioeconomy. *Front. Mar. Sci.* 7, 1247.
881 <https://doi.org/10.3389/FMARS.2020.626389/BIBTEX>
- 882 2. Bhattacharya, M., Goswami, S., 2020. Microalgae – A green multi-product
883 biorefinery for future industrial prospects. *Biocatal. Agric. Biotechnol.* 25,
884 101580. <https://doi.org/10.1016/J.BCAB.2020.101580>

- 885 3. Branco-Vieira, M., Martin, S.S., Agurto, C., Freitas, M.A.V., Mata, T.M.,
886 Martins, A.A., Caetano, N., 2018. Phaeodactylum tricornutum derived biosilica
887 purification for energy applications. Energy Procedia 153, 279–283.
888 <https://doi.org/10.1016/J.EGYPRO.2018.10.020>
- 889 4. Branco-Vieira, M., San Martin, S., Agurto, C., Freitas, M.A.V., Martins, A.A.,
890 Mata, T.M., Caetano, N.S., 2020. Biotechnological potential of Phaeodactylum
891 tricornutum for biorefinery processes. Fuel 268, 117357.
892 <https://doi.org/10.1016/J.FUEL.2020.117357>
- 893 5. Butler, T., Kapoore, R.V., Vaidyanathan, S., 2020. Phaeodactylum tricornutum:
894 A Diatom Cell Factory. Trends Biotechnol. 38, 606–622.
895 <https://doi.org/10.1016/J.TIBTECH.2019.12.023>
- 896 6. Butler, T.O., Padmaperuma, G., Lizzul, A.M., McDonald, J., Vaidyanathan, S.,
897 2022. Towards a Phaeodactylum tricornutum biorefinery in an outdoor UK
898 environment. Bioresour. Technol. 344, 126320.
899 <https://doi.org/10.1016/j.biortech.2021.126320>
- 900 7. Caballero, M.A., Jallet, D., Shi, L., Rithner, C., Zhang, Y., Peers, G., 2016.
901 Quantification of chrysolaminarin from the model diatom Phaeodactylum
902 tricornutum. Algal Res. 20, 180–188. <https://doi.org/10.1016/j.algal.2016.10.008>
- 903 8. Cerón-García, M.C., Fernández-Sevilla, J.M., Sánchez-Mirón, A., García-
904 Camacho, F., Contreras-Gómez, A., Molina-Grima, E., 2013. Mixotrophic
905 growth of Phaeodactylum tricornutum on fructose and glycerol in fed-batch and
906 semi-continuous modes. Bioresour. Technol. 147, 569–576.
907 <https://doi.org/10.1016/j.biortech.2013.08.092>
- 908 9. Cerón-García, M.C., Fernández Sevilla, J.M., Acién Fernández, F.G., Molina

- 909 Grima, E., García Camacho, F., 2000. Mixotrophic growth of *Phaeodactylum*
910 *tricornutum* on glycerol: Growth rate and fatty acid profile. *J. Appl. Phycol.* 12,
911 239–248. <https://doi.org/10.1023/a:1008123000002>
- 912 10. Cerón-García, M.C., Sánchez Mirón, A., Fernández Sevilla, J.M., Molina
913 Grima, E., García Camacho, F., 2005. Mixotrophic growth of the microalga
914 *Phaeodactylum tricornutum*: Influence of different nitrogen and organic carbon
915 sources on productivity and biomass composition. *Process Biochem.* 40, 297–
916 305. <https://doi.org/10.1016/j.procbio.2004.01.016>
- 917 11. Chauton, M.S., Olsen, Y., Vadstein, O., 2013. Biomass production from the
918 microalga *Phaeodactylum tricornutum*: Nutrient stress and chemical
919 composition in exponential fed-batch cultures. *Biomass and Bioenergy* 58, 87–
920 94. <https://doi.org/10.1016/j.biombioe.2013.10.004>
- 921 12. Enzing, C., Ploeg, M., Barbosa, M., Sijtsma, L., 2014. Microalgae-based
922 products for the food and feed sector: an outlook for Europe, JRC Scientific and
923 policy reports. <https://doi.org/10.2791/3339>
- 924 13. Eppink, M.H.M., Ventura, S.P.M., Coutinho, J.A.P., Wijffels, R.H., 2021.
925 Multiproduct Microalgae Biorefineries Mediated by Ionic Liquids. *Trends*
926 *Biotechnol.* <https://doi.org/10.1016/J.TIBTECH.2021.02.009>
- 927 14. Fernández Sevilla, J.M., Cerón García, M.C., Sánchez Mirón, A., Belarbi, E.H.,
928 García Camacho, F., Molina Grima, E., 2004. Pilot-Plant-Scale Outdoor
929 Mixotrophic Cultures of *Phaeodactylum tricornutum* Using Glycerol in Vertical
930 Bubble Column and Airlift Photobioreactors: Studies in Fed-Batch Mode.
931 *Biotechnol. Prog.* 20, 728–736. <https://doi.org/10.1021/BP034344F>
- 932 15. Francius, G., Tesson, B., Dague, E., Martin-Jézéquel, V., Dufrêne, Y.F., 2008.

- 933 Nanostructure and nanomechanics of live *Phaeodactylum tricornutum*
934 morphotypes. *Environ. Microbiol.* 10, 1344–1356.
935 <https://doi.org/10.1111/J.1462-2920.2007.01551.X>
- 936 16. Gallego, R., Montero, L., Cifuentes, A., Ibáñez, E., Herrero, M., 2018. Green
937 Extraction of Bioactive Compounds from Microalgae. *J. Anal. Test.* 2018 22 2,
938 109–123. <https://doi.org/10.1007/S41664-018-0061-9>
- 939 17. Gao, B., Chen, A., Zhang, W., Li, A., Zhang, C., 2017. Co-production of lipids,
940 eicosapentaenoic acid, fucoxanthin, and chrysolaminarin by *Phaeodactylum*
941 *tricornutum* cultured in a flat-plate photobioreactor under varying nitrogen
942 conditions. *J. Ocean Univ. China* 2017 165 16, 916–924.
943 <https://doi.org/10.1007/S11802-017-3174-2>
- 944 18. Gilbert-López, B., Barranco, A., Herrero, M., Cifuentes, A., Ibáñez, E., 2017.
945 Development of new green processes for the recovery of bioactives from
946 *Phaeodactylum tricornutum*. *Food Res. Int.* 99, 1056–1065.
947 <https://doi.org/10.1016/j.foodres.2016.04.022>
- 948 19. Gilbert-López, B., Mendiola, J.A., Fontecha, J., Broek, L.A.M. van den, Sijtsma,
949 L., Cifuentes, A., Herrero, M., Ibáñez, E., 2015. Downstream processing of
950 *Isochrysis galbana*: a step towards microalgal biorefinery. *Green Chem.* 17,
951 4599–4609. <https://doi.org/10.1039/C5GC01256B>
- 952 20. Gómez-Loredo, A., Benavides, J., Rito-Palomares, M., 2016. Growth kinetics
953 and fucoxanthin production of *Phaeodactylum tricornutum* and *Isochrysis*
954 *galbana* cultures at different light and agitation conditions. *J. Appl. Phycol.* 28,
955 849–860. <https://doi.org/10.1007/s10811-015-0635-0>
- 956 21. Günerken, E., D'Hondt, E., Eppink, M.H.M., Garcia-Gonzalez, L., Elst, K.,

- 957 Wijffels, R.H., 2015. Cell disruption for microalgae biorefineries. *Biotechnol.*
958 *Adv.* 33, 243–260. <https://doi.org/10.1016/J.BIOTECHADV.2015.01.008>
- 959 22. He, L., Han, X., Yu, Z., 2014. A Rare *Phaeodactylum tricornutum* Cruciform
960 Morphotype: Culture Conditions, Transformation and Unique Fatty Acid
961 Characteristics. *PLoS One* 9, e93922.
962 <https://doi.org/10.1371/JOURNAL.PONE.0093922>
- 963 23. Hockin, N.L., Mock, T., Mulholland, F., Kopriva, S., Malin, G., 2012. The
964 Response of Diatom Central Carbon Metabolism to Nitrogen Starvation Is
965 Different from That of Green Algae and Higher Plants. *Plant Physiol.* 158, 299–
966 312. <https://doi.org/10.1104/PP.111.184333>
- 967 24. Huete-Ortega, M., Okurowska, K., Kapoore, R.V., Johnson, M.P., Gilmour,
968 D.J., Vaidyanathan, S., 2018. Effect of ammonium and high light intensity on
969 the accumulation of lipids in *Nannochloropsis oceanica* (CCAP 849/10) and
970 *Phaeodactylum tricornutum* (CCAP 1055/1). *Biotechnol. Biofuels* 11, 1–15.
971 <https://doi.org/10.1186/s13068-018-1061-8>
- 972 25. Jallet, D., Caballero, M.A., Gallina, A.A., Youngblood, M., Peers, G., 2016.
973 Photosynthetic physiology and biomass partitioning in the model diatom
974 *Phaeodactylum tricornutum* grown in a sinusoidal light regime. *Algal Res.* 18,
975 51–60. <https://doi.org/10.1016/J.ALGAL.2016.05.014>
- 976 26. Kadalag, N.L., Pawar, P.R., Prakash, G., 2021. Co-cultivation of *Phaeodactylum*
977 *tricornutum* and *Aurantiochytrium limacinum* for polyunsaturated omega-3 fatty
978 acids production. *Bioresour. Technol.* 346, 126544.
979 <https://doi.org/10.1016/j.biortech.2021.126544>
- 980 27. Kooistra, W.H.C.F., Gersonde, R., Medlin, L.K., Mann, D.G., 2007. The Origin

981 and Evolution of the Diatoms: Their Adaptation to a Planktonic Existence. *Evol.*
982 *Prim. Prod. Sea* 207–249. <https://doi.org/10.1016/B978-012370518-1/50012-6>

983 28. Kroth, P.G., Chiovitti, A., Gruber, A., Martin-Jezeque, V., Mock, T., Parker,
984 M.S., Stanley, M.S., Kaplan, A., Caron, L., Weber, T., Maheswari, U.,
985 Armbrust, E.V., Bowler, C., 2008. A model for carbohydrate metabolism in the
986 diatom *Phaeodactylum tricornutum* deduced from comparative whole genome
987 analysis. *PLoS One* 3. <https://doi.org/10.1371/journal.pone.0001426>

988 29. Kuczynska, P., Jemiola-Rzeminska, M., Nowicka, B., Jakubowska, A., Strzalka,
989 W., Burda, K., Strzalka, K., 2020. The xanthophyll cycle in diatom
990 *Phaeodactylum tricornutum* in response to light stress. *Plant Physiol. Biochem.*
991 152, 125–137. <https://doi.org/10.1016/j.plaphy.2020.04.043>

992 30. Malviya, S., Scalco, E., Audic, S., Vincent, F., Veluchamy, A., Poulain, J.,
993 Wincker, P., Iudicone, D., De Vargas, C., Bittner, L., Zingone, A., Bowler, C.,
994 2016. Insights into global diatom distribution and diversity in the world’s ocean.
995 *Proc. Natl. Acad. Sci. U. S. A.* 113, E1516–E1525.
996 <https://doi.org/10.1073/PNAS.1509523113/-/DCSUPPLEMENTAL>

997 31. McClure, D.D., Luiz, A., Gerber, B., Barton, G.W., Kavanagh, J.M., 2018. An
998 investigation into the effect of culture conditions on fucoxanthin production
999 using the marine microalgae *Phaeodactylum tricornutum*. *Algal Res.* 29, 41–48.
1000 <https://doi.org/10.1016/j.algal.2017.11.015>

1001 32. McDowell, D., Dick, J.T., Eagling, L., Julius, M., Sheldrake, G.N.,
1002 Theodoridou, K., Walsh, P.J., 2020. Recycling nutrients from anaerobic
1003 digestates for the cultivation of *Phaeodactylum tricornutum*: A feasibility study.
1004 *Algal Res.* 48, 101893. <https://doi.org/10.1016/j.algal.2020.101893>

- 1005 33. Murchie, E.H., Lawson, T., 2013. Chlorophyll fluorescence analysis: A guide to
1006 good practice and understanding some new applications. *J. Exp. Bot.* 64, 3983–
1007 3998. <https://doi.org/10.1093/jxb/ert208>
- 1008 34. Not, F., Siano, R., Kooistra, W.H.C.F., Simon, N., Vaultot, D., Probert, I., 2012.
1009 Diversity and Ecology of Eukaryotic Marine Phytoplankton, *Advances in*
1010 *Botanical Research*. Elsevier. [https://doi.org/10.1016/B978-0-12-391499-](https://doi.org/10.1016/B978-0-12-391499-6.00001-3)
1011 [6.00001-3](https://doi.org/10.1016/B978-0-12-391499-6.00001-3)
- 1012 35. Penhaul Smith, J.K., Hughes, A.D., McEvoy, L., Day, J.G., 2020. Tailoring of
1013 the biochemical profiles of microalgae by employing mixotrophic cultivation.
1014 *Bioresour. Technol. Reports* 9, 100321.
1015 <https://doi.org/10.1016/j.biteb.2019.100321>
- 1016 36. Pereira, H., Sá, M., Maia, I., Rodrigues, A., Teles, I., Wijffels, R.H., Navalho, J.,
1017 Barbosa, M., 2021. Fucoxanthin production from *Tisochrysis lutea* and
1018 *Phaeodactylum tricornutum* at industrial scale. *Algal Res.* 56, 102322.
1019 <https://doi.org/10.1016/J.ALGAL.2021.102322>
- 1020 37. Qiao, H., Cong, C., Sun, C., Li, B., Wang, J., Zhang, L., 2016. Effect of culture
1021 conditions on growth, fatty acid composition and DHA/EPA ratio of
1022 *Phaeodactylum tricornutum*. *Aquaculture* 452, 311–317.
1023 <https://doi.org/10.1016/j.aquaculture.2015.11.011>
- 1024 38. Rodolfi, L., Biondi, N., Guccione, A., Bassi, N., D’Ottavio, M., Arganaraz, G.,
1025 Tredici, M.R., 2017. Oil and eicosapentaenoic acid production by the diatom
1026 *Phaeodactylum tricornutum* cultivated outdoors in Green Wall Panel (GWP®)
1027 reactors. *Biotechnol. Bioeng.* 114, 2204–2210.
1028 <https://doi.org/10.1002/BIT.26353>

- 1029 39. Savio, S., Farrotti, S., Paris, D., Arnaiz, E., Díaz, I., Bolado, S., Muñoz, R.,
1030 Rodolfo, C., Congestri, R., 2020. Value-added co-products from biomass of the
1031 diatoms *Staurosirella pinnata* and *Phaeodactylum tricornutum*. *Algal Res.* 47,
1032 101830. <https://doi.org/10.1016/J.ALGAL.2020.101830>
- 1033 40. Silva Benavides, A.M., Torzillo, G., Kopecký, J., Masojídek, J., 2013.
1034 Productivity and biochemical composition of *Phaeodactylum tricornutum*
1035 (*Bacillariophyceae*) cultures grown outdoors in tubular photobioreactors and
1036 open ponds. *Biomass and Bioenergy* 54, 115–122.
1037 <https://doi.org/10.1016/j.biombioe.2013.03.016>
- 1038 41. Simonazzi, M., Pezzolesi, L., Guerrini, F., Vanucci, S., Samorì, C., Pistocchi,
1039 R., 2019. Use of waste carbon dioxide and pre-treated liquid digestate from
1040 biogas process for *Phaeodactylum tricornutum* cultivation in photobioreactors
1041 and open ponds. *Bioresour. Technol.* 292, 121921.
1042 <https://doi.org/10.1016/J.BIORTECH.2019.121921>
- 1043 42. Song, M., Pei, H., Hu, W., Han, F., Ji, Y., Ma, G., Han, L., 2014. Growth and
1044 lipid accumulation properties of microalgal *Phaeodactylum tricornutum* under
1045 different gas liquid ratios. *Bioresour. Technol.* 165, 31–37.
1046 <https://doi.org/10.1016/j.biortech.2014.03.070>
- 1047 43. Song, Z., Lye, G.J., Parker, B.M., 2020. Morphological and biochemical
1048 changes in *Phaeodactylum tricornutum* triggered by culture media: Implications
1049 for industrial exploitation. *Algal Res.* 47, 101822.
1050 <https://doi.org/10.1016/J.ALGAL.2020.101822>
- 1051 44. Su, M., D’Imporzano, G., Veronesi, D., Afric, S., Adani, F., 2020.
1052 *Phaeodactylum tricornutum* cultivation under mixotrophic conditions with

1053 glycerol supplied with ultrafiltered digestate: A simple biorefinery approach
1054 recovering C and N. *J. Biotechnol.* 323, 73–81.
1055 <https://doi.org/10.1016/j.jbiotec.2020.07.018>

1056 45. Sun, J., Zhou, C., Cheng, P., Zhu, J., Hou, Y., Li, Y., Zhang, J., Yan, X., 2022.
1057 A simple and efficient strategy for fucoxanthin extraction from the microalga
1058 *Phaeodactylum tricornutum*. *Algal Res.* 61, 102610.
1059 <https://doi.org/10.1016/j.algal.2021.102610>

1060 46. Tesson, B., Gaillard, C., Martin-Jézéquel, V., 2009. Insights into the
1061 polymorphism of the diatom *Phaeodactylum tricornutum* Bohlin. *Bot. Mar.* 52,
1062 104–116. <https://doi.org/10.1515/BOT.2009.012>

1063 47. Tommasi, E., Cravotto, G., Galletti, P., Grillo, G., Mazzotti, M., Sacchetti, G.,
1064 Samorì, C., Tabasso, S., Tacchini, M., Tagliavini, E., 2017. Enhanced and
1065 Selective Lipid Extraction from the Microalga *P. tricornutum* by Dimethyl
1066 Carbonate and Supercritical CO₂ Using Deep Eutectic Solvents and Microwaves
1067 as Pretreatment. *ACS Sustain. Chem. Eng.* 5, 8316–8322.
1068 https://doi.org/10.1021/ACSSUSCHEMENG.7B02074/SUPPL_FILE/SC7B020
1069 [74_SI_001.PDF](https://doi.org/10.1021/ACSSUSCHEMENG.7B02074/SUPPL_FILE/SC7B020)

1070 48. Villanova, V., Fortunato, A.E., Singh, D., Bo, D.D., Conte, M., Obata, T.,
1071 Jouhet, J., Fernie, A.R., Marechal, E., Falciatore, A., Pagliardini, J., Le Monnier,
1072 A., Poolman, M., Curien, G., Petroustos, D., Finazzi, G., 2017. Investigating
1073 mixotrophic metabolism in the model diatom *phaeodactylum tricornutum*.
1074 *Philos. Trans. R. Soc. B Biol. Sci.* 372. <https://doi.org/10.1098/rstb.2016.0404>

1075 49. Villanova, V., Singh, D., Pagliardini, J., Fell, D., Le Monnier, A., Finazzi, G.,
1076 Poolman, M., 2021. Boosting Biomass Quantity and Quality by Improved

- 1077 Mixotrophic Culture of the Diatom *Phaeodactylum tricornutum*. *Front. Plant*
1078 *Sci.* 0, 411. <https://doi.org/10.3389/FPLS.2021.642199>
- 1079 50. Wang, S., Said, I.H., Thorstenson, C., Thomsen, C., Ullrich, M.S., Kuhnert, N.,
1080 Thomsen, L., 2018. Pilot-scale production of antibacterial substances by the
1081 marine diatom *Phaeodactylum tricornutum* Bohlin. *Algal Res.* 32, 113–120.
1082 <https://doi.org/10.1016/j.algal.2018.03.014>
- 1083 51. Wang, X.W., Huang, L., Ji, P.Y., Chen, C.P., Li, X.S., Gao, Y.H., Liang, J.R.,
1084 2019. Using a mixture of wastewater and seawater as the growth medium for
1085 wastewater treatment and lipid production by the marine diatom *Phaeodactylum*
1086 *tricornutum*. *Bioresour. Technol.* 289, 121681.
1087 <https://doi.org/10.1016/j.biortech.2019.121681>
- 1088 52. Wang, Z., Mou, J., Qin, Z., He, Y., Sun, Z., Wang, X., Sze Ki Lin, C., 2021. An
1089 auxin-like supermolecule to simultaneously enhance growth and cumulative
1090 eicosapentaenoic acid production in *Phaeodactylum tricornutum*. *Bioresour.*
1091 *Technol.* 345, 126564. <https://doi.org/10.1016/j.biortech.2021.126564>
- 1092 53. Yodsuwan, N., Sawayama, S., Sirisansaneeyakul, S., 2017. Effect of nitrogen
1093 concentration on growth, lipid production and fatty acid profiles of the marine
1094 diatom *Phaeodactylum tricornutum*. *Agric. Nat. Resour.* 51, 190–197.
1095 <https://doi.org/10.1016/j.anres.2017.02.004>
- 1096 54. Zhang, R., Lebovka, N., Marchal, L., Vorobiev, E., Grimi, N., 2020. Multistage
1097 aqueous and non-aqueous extraction of bio-molecules from microalga
1098 *Phaeodactylum tricornutum*. *Innov. Food Sci. Emerg. Technol.* 62, 102367.
1099 <https://doi.org/10.1016/J.IFSET.2020.102367>
- 1100 55. Zhang, W., Wang, F., Gao, B., Huang, L., Zhang, C., 2018. An integrated

1101 biorefinery process: Stepwise extraction of fucoxanthin, eicosapentaenoic acid
1102 and chrysolaminarin from the same *Phaeodactylum tricornutum* biomass. *Algal*
1103 *Res.* 32, 193–200. <https://doi.org/10.1016/j.algal.2018.04.002>
1104 56. Zhou, X., Jin, W., Tu, R., Guo, Q., Han, S. fang, Chen, C., Wang, Qing, Liu,
1105 W., Jensen, P.D., Wang, Qilin, 2019. Optimization of microwave assisted lipid
1106 extraction from microalga *Scenedesmus obliquus* grown on municipal
1107 wastewater. *J. Clean. Prod.* 221, 502–508.
1108 <https://doi.org/10.1016/J.JCLEPRO.2019.02.260>
1109